Int. J. Multiphase Flow Vol. 19, No. 2, pp. 347–367, 1993
Printed in Great Britain.

0301-9322/93 $6.00 + 0.00

A LAGRANGIAN MODEL FOR SOLID PARTICLES IN TURBULENT FLOWS

Q. Q. LU,† J. R. FONTAINE and G. AUBERTIN
Institut National de Recherche et de Sécurité, Avenue de Bourgogne, 54501 Vandoeuvre Cédex, France

(Received 14 March 1991; in revised form 30 November 1992)

Abstract—Applying the time series analysis idea to the temporal and spatial fluid velocity correlations, a three-dimensional Lagrangian model for the motion of particles in turbulent flows has been established. This model has been used to simulate the experiments of other workers. The computed results are compared with the experimental data for the particle dispersion, velocity correlations and velocity decay. In the case where the mean turbulent flow has one main direction, this model has been extended to include the Eulerian temporal velocity correlation; a so-called mixed model has been devised. This model has been used to compute particle dispersion in stationary, homogeneous, isotropic and incompressible turbulence. Comparison is made with the theroetical long-time particle diffusion coefficients for cases where the crossing-trajectory effect is important or unimportant. Good agreement is obtained.

Key Words: Lagrangian model, particles, turbulence

1. INTRODUCTION

A number of computational methods have been developed to describe turbulent flows laden with particles. These methods use either Eulerian or Lagrangian analyses. In the Eulerian approach, both the fluid carrier and the particulate phase are assumed to be continuous media and sets of coupled differential equations are derived for each phase (e.g. Abbas *et al.* 1980; Durst *et al.* 1984; Elghobashi *et al.* 1984). In the Lagrangian approach, particles are treated individually by solving the dynamic equation of particle motion and the bulk properties of the particulate phase are obtained by averaging over a statistically significant number of particles.

This paper models particle motion in turbulence by a Lagrangian method. Gosman & Ioannides (1981) proposed a model to account for the effect of fluid turbulence on particles when the mean fluid velocity is known and the fluctuating part is obtained by sampling from a Gaussian probability distribution function (p.d.f.) whose variance is proportional to the local turbulent kinetic energy. The dynamic equation of particle motion is integrated with the fluid instantaneous velocity unchanged until a particle–eddy interaction time expires. This particle–eddy interaction time is defined to be the minimum of the eddy lifetime and the transit time. In this model, the turbulent instantaneous velocity field is supposed to be uniform within the eddy. In other words, this model does not account for the continuity effect (Csanady 1963) which leads to a difference between the particle longitudinal and transverse long-time diffusion coefficients (Csanady 1963; Reeks 1977; Nir & Pismen 1979). Shuen *et al.* (1983, 1985) used the same idea. Kallio & Reeks (1989) modified this model by determining the eddy lifetime with an exponential p.d.f. distribution having the mean equal to the Lagrangian integral timescale. Burnage & Moon (1990) advanced further in this direction. Their model contains both a random timescale and a random lengthscale. The dynamic equation of particle motion was integrated with the fluid instantaneous velocity unchanged until either the integrating time or the distance between the particle and a fluid point is greater than the corresponding random scale. The two random scales are given by random selections from two Poisson processes whose means are the turbulent Lagrangian integral timescale and the eddy lengthscale.

Ormancey & Martinon (1984) introduced another way of modeling particle motion in turbulent flows. They constructed a sampling process for the fluctuating velocity of a fluid point during a finite interval of time. For the fluctuating velocity of the fluid at the particle position however, they

†Present address: Department of Chemical & Nuclear Engineering, The University of California, Santa Barbara, CA 93106, U.S.A.

used another random process which accounts for the fluid Eulerian longitudinal and transverse correlations. As a result, this model includes the continuity effect on particle dispersion. They followed, simultaneously, a particle and a fluid point until the distance between them exceeds a certain given lengthscale. Berlemont *et al.* (1990) pursued this approach but expressed the fluctuating fluid velocity along the fluid trajectory as the weighted sum of its past values plus a random variable, as suggested by Parthasarathy & Faeth (1990). These two models followed a fluid point during a finite time interval and used noise terms in the temporal and spatial correlation relations that are mean-zero, Gaussian variables.

The starting point of the present study is the time series analysis idea (Box & Jenkins 1976). By applying it to both the fluid Lagrangian and the Eulerian spatial correlations, the fluctuating fluid velocities at two successive positions of the particle are specified. In the present model, the fluid location and velocity change at every time step. The correlation functions are specified only for one time step of computation, Δt, and for the distance developed between the particle and a fluid point during Δt. An appropriate linear combination of noise terms is used so that they are mean-zero, Gaussian variables.

This paper is organized as follows. Section 2 is devoted to the establishment of model 1. The choice of the correlation functions and the associated parameters are discussed in subsection 3.1. The predicted results for particle dispersion, for the decay of fluctuating velocity and for the velocity correlation are compared with experimental data of Snyder & Lumley (1971) and of Wells & Stock (1983) in subsections 3.2 and 3.3. In subsection 3.2, a comparison is also made with the theoretical results of Nir & Pismen (1979) for velocity correlations of the copper particle of the experiment of Snyder & Lumley. The sensitivity of model 1 to the time step and a numerical parameter is examined in subsection 3.4. In subsection 3.5, an extension of model 1 is introduced that incorporates the Eulerian temporal velocity correlation. This establishes model 2 (the mixed model). This model is applied to particle dispersion in a stationary, homogeneous, isotropic and incompressible turbulent flow. The predicted long-time particle diffusion coefficients are compared with the theoretical results of Csanady (1963), Nir & Pismen (1979) and Pismen & Nir (1978), both in the presence and the absence of the crossing-trajectory effect.

2. ESTABLISHMENT OF THE METHOD

2.1. Particle motion

The present study neglects the Basset term and the temporal derivatives of the fluctuating fluid velocity along the trajectories of solid and fluid particles. Such a simplification has been justified for low turbulence intensities and moderate departure from homogeneity (Ormancey 1984). The corresponding derivatives of the fluid mean velocity, however, are preserved. By neglecting the influence of streamline curvature and the interaction between particles, the motion of a spherical and rigid particle is presented by the following equations:

$$\rho_p \frac{d\mathbf{V}}{dt} = -\frac{3}{4d_p}\rho_f C_D(\mathbf{V}-\mathbf{U})|\mathbf{V}-\mathbf{U}| - 0.5\rho_f \frac{d(\mathbf{V}-\mathbf{U})}{dt} + (\rho_p - \rho_f)\mathbf{g} \quad [1]$$

and

$$\frac{d\mathbf{X}}{dt} = \mathbf{V} \quad [2]$$

where ρ_p and ρ_f are the particle and fluid densities, respectively, $\mathbf{V}$ and $\mathbf{U}$ are the instantaneous velocities of particles and fluid, respectively, d_p is the particle diameter and $\mathbf{g}$ is the gravitational acceleration. The coefficient C_D is introduced for the drag term and is given by

$$C_D = \frac{24}{(\mathrm{Re})_p}[1 + 0.15(\mathrm{Re})_p^{0.687}] \quad \text{for } (\mathrm{Re})_p < 200,$$

where $(\mathrm{Re})_p$, the particle Reynolds number, is defined as

$$(\mathrm{Re})_p = \frac{|\mathbf{U}-\mathbf{V}|d_p}{\nu}.$$

In this study, the lift forces, due to either particle rotation (Rubinow & Keller 1961) or to fluid velocity gradient (Saffman 1965), are not included, but the virtual mass term is.

The effect of fluid turbulence on the particles is considered but the modification of the turbulent field due to the presence of particles is ignored. Therefore, all the mean data of the fluid field, including the mean velocity, the mean turbulent kinetic energy and the mean turbulent kinetic energy dissipation rate, are regarded as known *a priori*. They could be obtained by measurements or by a turbulent model. To know the statistic properties of particles, each particle is followed along its trajectory by integrating [1] and [2]. To do this, it is necessary to know the instantaneous velocity of the fluid at the location points of the particle. Since the fluid mean velocity is supposed to be known, it is only necessary to estimate the fluctuating fluid velocity at the location point of the particle.

2.2. Model 1

At the instant t, the particle and a fluid particle start out from the same position $\mathbf{X}_s$. After one time step of computation, Δt, they arrive at $\mathbf{X}_p$ and $\mathbf{X}_f$, respectively, and the distance between $\mathbf{X}_p$ and $\mathbf{X}_f$ is Δs, as shown in figure 1. A relative coordinate system O–$\Theta\Xi\Omega$ is defined. The relative coordinate system O–$\Theta\Xi\Omega$ is chosen such that its origin is located at $\mathbf{X}_f$ and the Θ axis passes through the two positions $\mathbf{X}_f$ and $\mathbf{X}_p$. Here $\mathbf{X}_s$, $\mathbf{X}_f$ and $\mathbf{X}_p$ are the position vectors in the absolute coordinate system o–xyz.

Since, in practical applications, flow fields are often non-homogeneous and non-stationary, the fluctuating velocity u_i is normalized by the square root of its local variance to lessen the effects of reference time and position. The normalized fluctuating component in the i-direction by W_i, i.e.

$$W_i = \frac{u_i}{\sqrt{\overline{u_i^2}}} \quad (i = 1, 2, 3),$$

where the subscripts 1, 2 and 3 represent, respectively, the directions of the relative Θ, Ξ and Ω axes. The quantities with overbars indicate the ensemble average values.

In the relative coordinate system O–$\Theta\Xi\Omega$, the normalized fluctuating velocities at positions $\mathbf{X}_s$, $\mathbf{X}_f$, $\mathbf{X}_p$ are assumed to have the following correlation relations:

$$\overline{W_i(\mathbf{X}_f)W_j(\mathbf{X}_s)} = \overline{W_i(\mathbf{X}_s)W_j(\mathbf{X}_s)}f_{ij}^L(\Delta t) \quad (i,j = 1, 2, 3) \qquad [3]$$

and

$$\overline{W_i(\mathbf{X}_p)W_j(\mathbf{X}_f)} = \overline{W_i(\mathbf{X}_f)W_j(\mathbf{X}_f)}g_{ij}(\Delta s) \quad (i,j = 1, 2, 3). \qquad [4]$$

Relations [3] and [4] are called, respectively, the Lagrangian auto-correlation and Eulerian spatial velocity correlation functions. It should be pointed that the two relations are postulated for one time step of calculation, Δt. Throughout this paper, no summation convention is used.

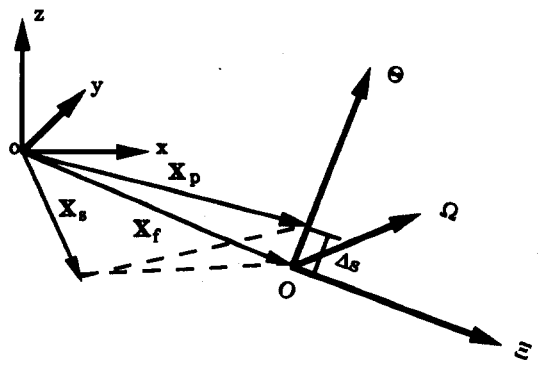

Figure 1. The locations of the particle and a fluid particle at the instants t and $t + \Delta t$.

Only the isotropic case is considered. The Reynolds stress components $\overline{u_i u_j}$ are, thus, zero for $i \neq j$ and the correlation relations [3] and [4] become:

$$\overline{W_i(\mathbf{X}_f)W_i(\mathbf{X}_s)} = \overline{W_i(\mathbf{X}_s)W_i(\mathbf{X}_s)} f_{ii}^{L}(\Delta t) \quad (i = 1, 2, 3) \tag{5}$$

and

$$\overline{W_i(X_p)W_i(\mathbf{X}_f)} = \overline{W_i(\mathbf{X}_f)W_i(\mathbf{X}_f)} g_{ii}(\Delta s) \quad (i = 1, 2, 3). \tag{6}$$

The idea of a time series analysis (Box & Jenkins 1976) is used for the stochastic process of the fluid point from $\mathbf{X}_s$ to $\mathbf{X}_f$. Thus,

$$W_i(\mathbf{X}_f) = a_i W_i(\mathbf{X}_s) + \alpha_i \quad (i = 1, 2, 3), \tag{7}$$

where a_i $(i = 1, 2, 3)$ are coefficients yet to be determined and α_i $(i = 1, 2, 3)$ are mean-zero, random variables independent of $W_i(\mathbf{X}_s)$ but not necessarily Gaussian, whose properties will be discussed later. To determine the coefficients a_i, the two sides of [7] are multiplied by $W_i(\mathbf{X}_s)$ and the ensemble average is taken. After accounting for the independence of α_i and $W_i(\mathbf{X}_s)$, the following relation is obtained:

$$\overline{W_i(\mathbf{X}_f)W_i(\mathbf{X}_s)} = a_i \overline{W_i(\mathbf{X}_s)W_i(\mathbf{X}_s)} \quad (i = 1, 2, 3). \tag{8}$$

Substitution of [5] into [8] gives

$$a_i = f_{ii}^{L}(\Delta t). \tag{9}$$

Squaring both sides of [7] and taking the ensemble average, the variance of α_i is determined to be

$$(\sigma_\alpha)_i = \sqrt{1 - a_i^2} \quad (i = 1, 2, 3).$$

It is evident from the definition of a_i that when $\mathbf{X}_f$ approaches $\mathbf{X}_s$, $a_i \to 1$ and thus $(\sigma_\alpha)_i \to 0$. In fact, if α_i is represented by a Gaussian white noise, for homogeneous turbulent flows, [7] will reduce to the equation used by Parthasarathy & Faeth (1990). Furthermore if a_i is represented by an exponential function, [7] will be identical to the equation of Kaplan & Dinan (1988) and if Δt is very small compared to the Lagrangian integral timescale, [7] will be equivalent to the Langevin equation (Wax 1954; Durbin 1980; Sawford & Hunt 1986). For the close similarity of [7] with the Langevin equation, the size of the computation time step Δt may be subjected to certain limitations (see Durbin 1980).

If the concept of a time series analysis is extended to represent the effect of spatial displacement on the fluctuating velocities of the fluid at the points $\mathbf{X}_f$ and $\mathbf{X}_p$,

$$W_i(\mathbf{X}_p) = b_i W_i(\mathbf{X}_f) + \beta_i \quad (i = 1, 2, 3), \tag{10}$$

where $b_i (i = 1, 2, 3)$ and β_i $(i = 1, 2, 3)$ has the same sense as a_i and α_i in [7]. By the procedure already adopted for [7], it is from [10] that

$$b_i = g_{ii}(\Delta s). \tag{11}$$

Introducing [7] into [10] to eliminate $W_i(\mathbf{X}_f)$,

$$W_i(\mathbf{X}_p) = a_i b_i W_i(\mathbf{X}_s) + \underline{b_i \alpha_i + \beta_i} \quad (i = 1, 2, 3). \tag{12}$$

Denoting the terms underlined in [12] by ψ_i, [12] can be rewritten as

$$W_i(\mathbf{X}_p) = a_i b_i W_i(\mathbf{X}_s) + \psi_i \quad (i = 1, 2, 3). \tag{13}$$

Here ψ_i $(i = 1, 2, 3)$ are assumed to be mean-zero, Gaussian random variables. To complete [13], the standard deviations $(\sigma_\psi)_i$ of ψ_i are needed. By squaring both sides of [13] and taking the ensemble average, assuming the independence of $W_i(\mathbf{X}_s)$ and ψ_i, the following is obtained:

$$(\sigma_\psi)_i = \sqrt{1 - a_i^2 b_i^2} \quad (i = 1, 2, 3). \tag{14}$$

Equation [13] together with [14] is called model 1. The method established above is based on the fluid Lagrangian temporal velocity correlation of the stochastic process representing the motion of the fluid particle from $\mathbf{X}_s$ to $\mathbf{X}_f$. It will be called the Lagrangian temporal construction.

In the present study, [13] is used as the model equation. It represents the fluctuating velocities of the fluid at successive locations of the particle and includes both the time and space effects of the turbulent field via the coefficients a_i and b_i. This model, in contrast to the conventional time series method, has no restriction that α_i and β_i are mean-zero, Gaussian variables. However, the requirement that the appropriate linear combination has these property, does place the restriction on the properties of α_i and β_i.

It is noted that the coordinate system employed in figure 1 is only established for one time step and it should be changed continuously in the course of computation.

2.3. The calculation procedures

(1) At $t = 0$, the particle position and velocity are given. The initial fluctuating fluid velocity components u_i $(i = 1, 2, 3)$ at the particle position are obtained from the Gaussian variables satisfying the p.d.f. with the local variances $\overline{u_i^2}$. The instantaneous fluid velocity can then be obtained by adding the known mean velocity and the fluctuating part.

(2) From the instantaneous fluid velocity found above, the fluid point position at time Δt, $\mathbf{X}_f$ can be calculated by the Euler–Cauchy method (referring to figure 1). Using the given particle initial velocity and the instantaneous fluid velocity just obtained, through [1] and [2], the position of the particle at the instant Δt, $\mathbf{X}_p$, is obtained by the Runge–Kutta method. Displacement Δs can then be calculated (see figure 1).

(3) Establish the relative coordinate system O–$\Theta\Xi\Omega$. From [9] and [11], the coefficients a_i and b_i in [13] are estimated. The random terms ψ_i having the standard deviations given by [14] are generated by computer with the aid of the software GASDEV (Vetterling *et al.* 1988). The fluctuating velocity of the fluid point at $\mathbf{X}_p$ (the new particle position computed at step 2) can be found from [13].

(4) Let $\mathbf{X}_p$ be the starting point, i.e. $\mathbf{X}_s$, for the next time step and repeat steps 2 and 3 until completion of the computation.

3. VERIFICATION OF MODEL 1

3.1. Choice of the correlation functions and the associated parameters

In what follows, the following forms of the temporal and spatial correlation functions proposed by Frenkiel (1948) are adopted:

$$\overline{W_i(\mathbf{X}_f)W_i(\mathbf{X}_s)} = \overline{W_i(\mathbf{X}_s)W_i(\mathbf{X}_s)}\exp\left(\frac{-\Delta t}{\tau_i^L}\right) \qquad (i = 1, 2, 3) \qquad [15]$$

and

$$\overline{W_i(\mathbf{X}_p)W_i(\mathbf{X}_f)} = \overline{W_i(\mathbf{X}_f)W_i(\mathbf{X}_f)}\exp\left(\frac{-\Delta s}{2\Lambda_i}\right)\cos\left(\frac{\Delta s}{2\Lambda_i}\right) \quad (i = 1, 2, 3). \qquad [16]$$

where Λ_1 is the longitudinal lengthscale and Λ_2 and Λ_3 are the transverse lengthscales. Of course, other forms of the correlation functions can be used to replace [16], e.g. exponential functions. In the present study, all the sample computations are conducted for isotropic and incompressible turbulence. Therefore, the Lagrangian integral timescales τ_i^L and Eulerian lengthscales Λ_i in [15] and [16] can be estimated by

$$\tau_1^L = \tau_2^L = \tau_3^L = \mathrm{Ce}_1\frac{\overline{u^2}}{\varepsilon}, \qquad [17]$$

$$\Lambda_1 = \mathrm{Ce}_2\tau_1^L\sqrt{\overline{u_i^2}} \qquad [18]$$

and

$$\Lambda_3 = \Lambda_2 = \mathrm{Ce}_3\Lambda_1, \qquad [19]$$

where $\overline{u^2} = \frac{1}{3}(\overline{u_1^2} + \overline{u_2^2} + \overline{u_3^2})$ are ε is the turbulent kinetic energy dissipation rate. Relations [17] and [18] can be found in Hinze (1975). According to Hinze (1975, p. 398), Ce_1 and Ce_2 are not independent but satisfy the following relation:

$$Ce_2 = \frac{0.588}{Ce_1}. \quad [20]$$

Again, based on the discussion of the theory of isotropic, incompressible turbulence by Hinze (1975, p. 426), $Ce_1 = 0.235$ and $Ce_3 = 0.5$. For convenience, the values of the associated parameters used throughout the present study are listed in table 1.

In cases of isotropic or weakly anisotropic turbulence, the following relations hold between the fluctuating fluid velocity variances in the absolute coordinate system o–xyz and in the relative coordinate system O–$\Theta\Xi\Omega$:

$$\overline{u_1^2} = l_1^2\overline{u_x^2} + m_1^2\overline{u_y^2} + n_1^2\overline{u_z^2} \quad [21]$$

$$\overline{u_2^2} = l_2^2\overline{u_x^2} + m_2^2\overline{u_y^2} + n_2^2\overline{u_z^2} \quad [22]$$

$$\overline{u_3^2} = l_3^2\overline{u_x^2} + m_3^2\overline{u_y^2} + n_3^2\overline{u_z^2}; \quad [23]$$

where l_1, m_1, n_1; l_2, m_2, n_2 and l_3, m_3, n_3 are the direction cosines of the Θ, Ξ and Ω axes relative to the x, y and z axes, respectively.

3.2. *Simulation of the experiment of Snyder & Lumley (1971)*

One of the most comprehensive experiments on particle motion in turbulent flows is that made by Snyder & Lumley (1973). With the use of a grid system, they produced a nearly isotropic decaying turbulent air flow (air density = 1.205×10^{-3} g/cm^3 and kinematic viscosity = 14.937×10^{-2} cm^2/s). The particles ranged from light particles which follow the turbulent flow to heavy particles which experience both inertia and crossing-trajectory effects. Their diameters, densities and kinematic viscosity are given in table 2. The particles were injected into the turbulent flow at $x/M = 20$. The measurement was carried at or beyond $x/M = 68$, where x represents the distance from the grid and the grid spacing $M = 2.54$ cm.

The principal direction of the flow was vertically upward. The experimental mean turbulence data are given by

$$\overline{U_x} = 655 \text{ (cm/s)}, \quad \overline{U_y} = 0, \quad \overline{U_z} = 0, \quad [24]$$

$$\overline{u_x^2} = \frac{(\overline{U_x})^2}{42.4\left(\frac{x}{M} - 16\right)}, \quad [25]$$

$$\overline{u_y^2} = \frac{(\overline{U_x})^2}{39.4\left(\frac{x}{M} - 12\right)} \quad [26]$$

and

$$\overline{u_z^2} = \overline{u_y^2}. \quad [27]$$

From Taylor's frozen hypothesis and the relation $dk/dt = -\varepsilon$, where k, the turbulent kinetic energy, is defined as

$$k = \tfrac{1}{2}(\overline{u_x^2} + \overline{u_y^2} + \overline{u_z^2}), \quad [28]$$

Table 1. Values of the associated coefficients and the time step Δt

Ce_1	Ce_2	Ce_3	Δt (s)
0.235	2.5	0.5	0.001

Table 2. Parameters of the particles used in the experiment of Snyder & Lumley (1971)

	Hollow glass	Corn pollen	Glass	Copper
Diameter (μm)	46.5	87.0	87.0	46.5
Density (g/cm^3)	0.26	1.00	2.50	8.90

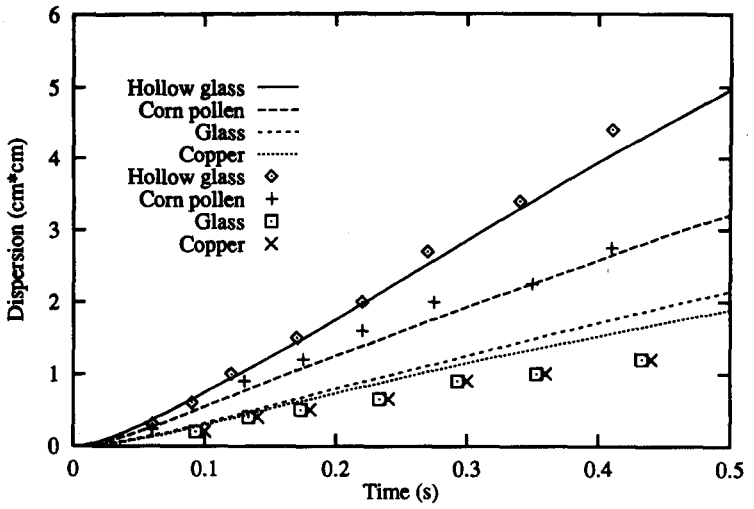

Figure 2a. Predicted and experimental particle transverse dispersions.

the turbulent kinetic energy dissipation rate is obtained as

$$\varepsilon = \frac{(\overline{U_x})^3}{2M}\left[\frac{1}{42.4\left(\frac{x}{M}-16\right)^2}+\frac{2}{39.4\left(\frac{x}{M}-12\right)^2}\right]. \qquad [29]$$

In all the following comparisons, the lines represent the computed results, while the symbols are experimental data. Figure 2a compares the predicted and experimental transverse particle dispersions. To examine the overall effect of gravity on particle dispersion, figure 2b shows the displacement of particles in the gravity direction (the x-direction in the study). The comparison in figure 2a is in a fair agreement, although appreciable differences are observed. A larger difference is noticed for heavy particles. The comparison suggests that the present model works for the hollow glass particle, for which some Lagrangian approaches fail (Ormancey & Martinon 1984; Berlemont *et al.* 1990). As predicted by previous studies (e.g. Reeks 1977), figure 2b implies that particles disperse quickly in the direction of gravity due to the continuity effect.

Figure 3a compares the numerical and experimental results on the decay of the transverse velocity fluctuation of the particles. Here the particle fluctuating velocity u is normalized by the square of the longitudinal mean velocity U [here 655 (cm/s)]. Qualitative agreement is noted but

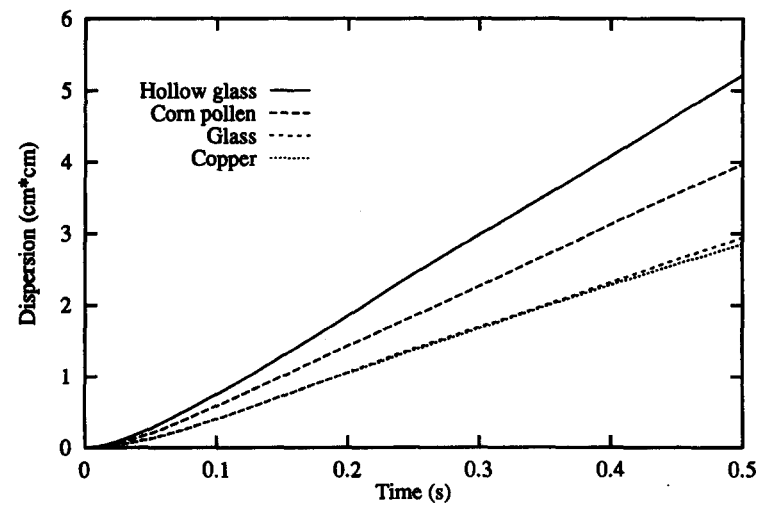

Figure 2b. Predicted particle longitudinal dispersions.

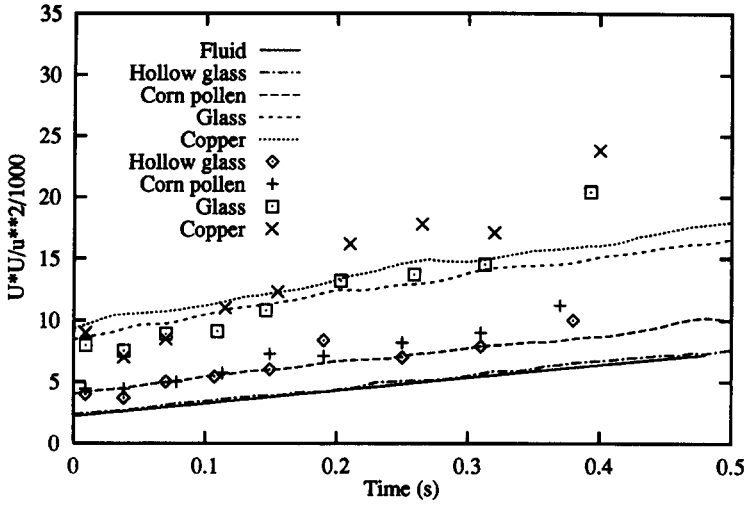

Figure 3a. Predicted and experimental transverse fluctuating particle velocity decays.

obvious differences appear, particularly for the hollow glass particles. This could be due to the low sampling rate used in the experiment. Figure 3(b) gives the predicted longitudinal fluctuating particle velocity decay. It shows that the fluctuating particle velocity decays more slowly in the gravity direction than in the normal direction. This is in agreement with the theoretical conclusion of other investigators (e.g. Reeks 1977).

For the reasons given by Nir & Pismen (1979), no attempt was made in this paper to compare the predicted results with Snyder & Lumley's (1971) particle velocity correlations. Figure 4, instead, compares the computed Lagrangian correlations of the copper particle transverse velocity along with the theoretical results of Nir & Pismen (1979). Reasonably good agreement is observed in figure 4, where x/M represents the location where the calculation was made of the correlation coefficient defined as below:

$$R_{ii}^{L}(\Delta t) = \frac{\overline{u_i(\Delta t)u_i(0)}}{\overline{u_i^2(0)}} \quad (i = x, y). \tag{30}$$

The Lagrangian correlation timescales are defined as

$$\tau_{ii} = \int_0^\infty R_{ii}^{L}(\varphi)\,\mathrm{d}\varphi \quad (i = x, y). \tag{31}$$

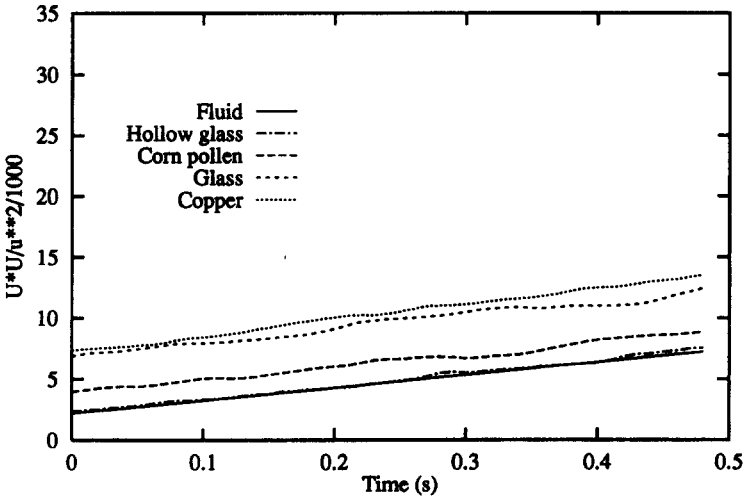

Figure 3b. Predicted longitudinal fluctuating particle velocity decays.

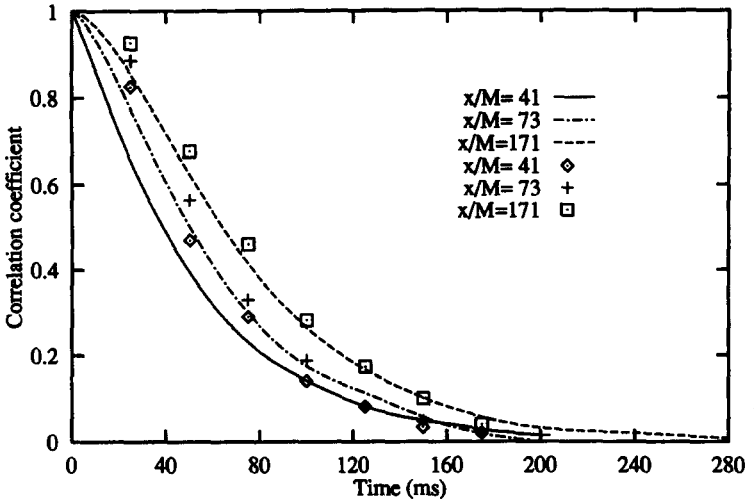

Figure 4. Comparison of the numerical and theoretical (Nir & Pismen 1979) Lagrangian correlations of the copper particle transverse velocity.

As we know, increasing particle inertia will reduce the particle fluctuating velocity. On the other hand, this will also lead to an increase in the particle correlation. For examining the latter, we calculate the longitudinal and transverse Lagrangian correlation coefficients of the particle fluctuating velocity. Since the particle dispersions in the experiment are symmetric relative to the x axis, only the velocity correlations for the x- and y-components are computed. The computation is performed at three sections, $x/M = 41$, 73 and 171. The integral timescales of these correlation are denoted by τ_{ii}^{p} $(i = x, y)$ and their computed values are tabulated in tables 3–6. It can be seen from these tables that the particle velocity correlates more in the direction of gravity than in the direction normal to it. As a result, the integral timescale is larger in the gravity direction than its counterpart in the normal direction. In tables 3–6, the timescale τ_{l}^{L} is computed by [17].

3.3. *Simulation of the experiment of Wells & Stock (1983)*

Wells & Stock (1983) used an identical grid system to Snyder & Lumley's (1971) to produce a turbulent air flow, but the main direction of the flow was horizontal. The mean data for the turbulent field are

$$\overline{U_x} = 655 \text{ (cm/s)}, \quad \overline{U_y} = 0, \quad \overline{U_z} = 0, \qquad [32]$$

$$\overline{u_x^2} = \frac{(\overline{U_x})^2}{53.224\left(\dfrac{x}{M} - 7.053\right)}, \qquad [33]$$

Table 3. Hollow glass particle

$\frac{x}{M}$	τ_{xx}^{p} (ms)	τ_{yy}^{p} (ms)	τ_{l}^{L} (ms)
41	14.93	15.83	16.68
73	36.82	38.82	36.21
171	95.39	96.70	95.79

Table 4. Corn Pollen particle

$\frac{x}{M}$	τ_{xx}^{p} (ms)	τ_{yy}^{p} (ms)	τ_{l}^{L} (ms)
41	29.90	29.88	16.68
73	42.60	39.55	36.21
171	80.62	64.62	95.79

Table 5. Glass particle

$\frac{x}{M}$	τ_{xx}^{p} (ms)	τ_{yy}^{p} (ms)	τ_{l}^{L} (ms)
41	41.07	50.96	16.68
73	60.69	61.55	36.21
171	85.11	72.30	95.79

Table 6. Copper

$\frac{x}{M}$	τ_{xx}^{p} (ms)	τ_{yy}^{p} (ms)	τ_{l}^{L} (ms)
41	53.86	56.23	16.68
73	63.13	62.95	36.21
171	90.13	77.25	95.79

$$\overline{u_y^2} = \frac{\overline{(U_x)^2}}{56.546\left(\frac{x}{M} - 8.867\right)} \quad [34]$$

and

$$\overline{u_z^2} = \overline{u_y^2}. \quad [35]$$

The turbulent kinetic energy dissipation rate is

$$\varepsilon = \frac{\overline{(U_x)}^3}{2M}\left[\frac{1}{53.224\left(\frac{x}{M} - 7.053\right)^2} + \frac{2}{56.546\left(\frac{x}{M} - 8.867\right)^2}\right]. \quad [36]$$

Here ε is obtained in the same way as the experiment of Snyder & Lumley (1971).

In this experiment, 5 and 57 μm glass particles were charged before the grid and an adjustable, uniform electrical field within the test section was used so as to change the resultant force acting on the particles and, therefore, the particle terminal velocity V_t. The densities of the 5 and 57 μm particles are 2.475 (g/cm^3) and 2.420 (g/cm^3), respectively. In this simulation, gravity is in the negative direction of the y axis and the main flow direction coincides with the x axis.

Figures 5 and 6 give the predicted and measured transverse dispersions for 5 and 57 μm particles, respectively. Reasonable agreement is observed when the particle terminal velocity V_t is relatively small. As V_t becomes larger, the computed and experimental data disagree considerably. In the experiment, the tendency for the 57 μm particles to disperse faster than the 5 μm particles when $V_t = 0$ was reported. This cannot be noted in the prediction data.

Figure 7a and 7b compare the predicted and experimental data of 5 μm particle fluctuating velocity decay in the longitudinal and transverse directions, i.e. in the x- and y-directions, respectively. Figures 8a and 8b show the results for the 57 μm particles. It is seen that the predicted results agree fairly well with the experimental data when V_t is not too large. As V_t gets larger, there is an apparent discrepancy and the agreement is worse. It can be noted that due to the continuity effect, the fluctuating particle velocities decay at different rates in the directions parallel and normal to gravity.

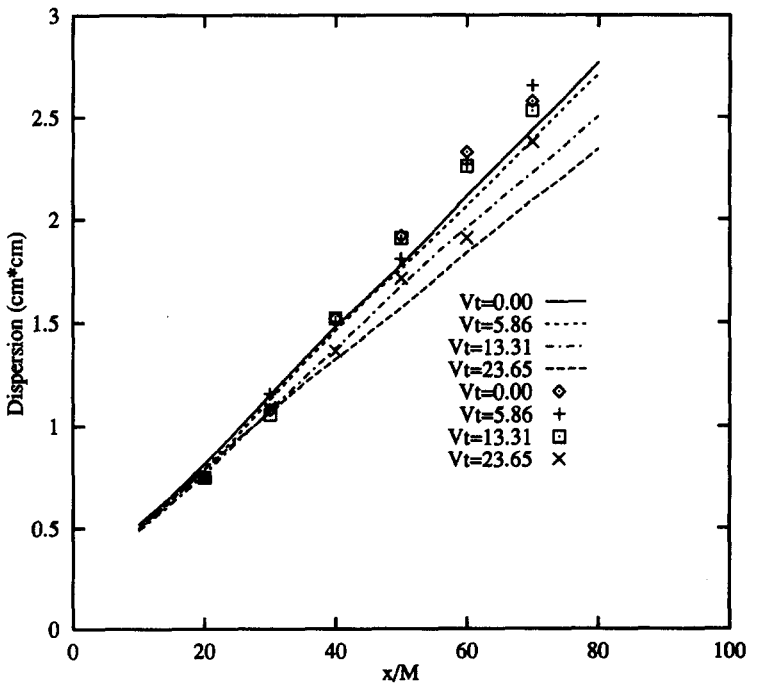

Figure 5. Predicted and experimental transverse dispersions of 5 μm particles.

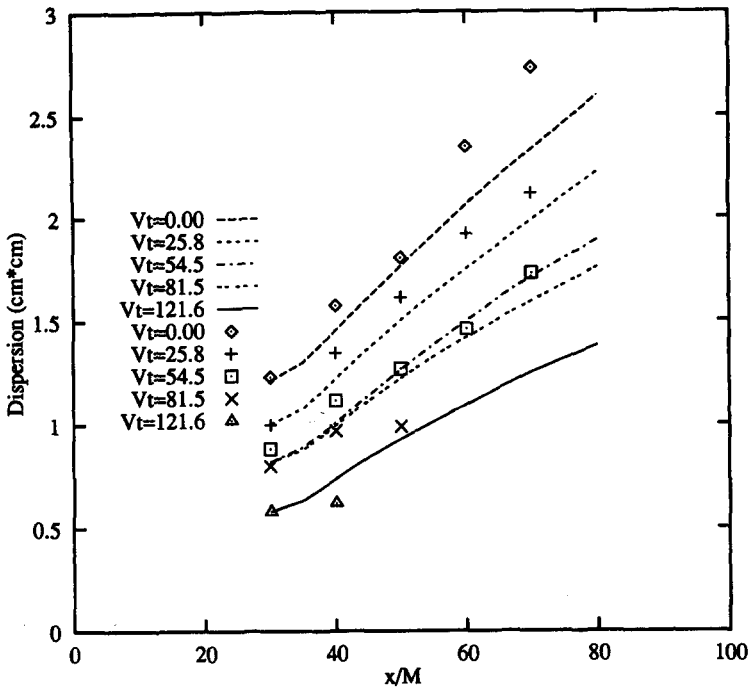

Figure 6. Predicted and experimental transverse dispersions of the 57 μm particles.

Figure 9a and 9b show the predicted Lagrangian particle velocity correlations in the longitudinal direction. According to the experimental information on the ratio of the Eulerian and Lagrangian timescales, we can deduce from the experimental data the Lagrangian particle velocity correlation in the longitudinal direction for the case of $V_t = 0$. The derived results are also plotted in figures 9a and 9b.

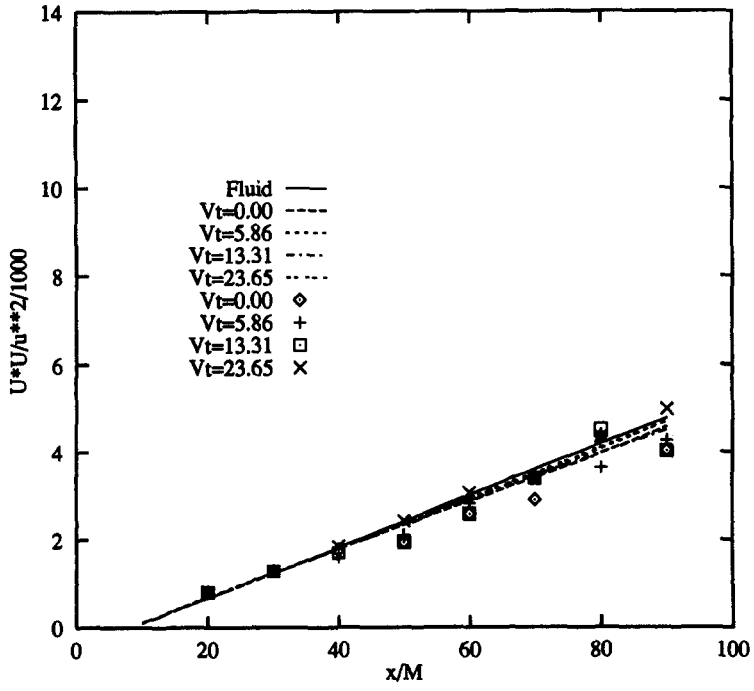

Figure 7a. Predicted and experimental longitudinal velocity decays of the 5 μm particles.

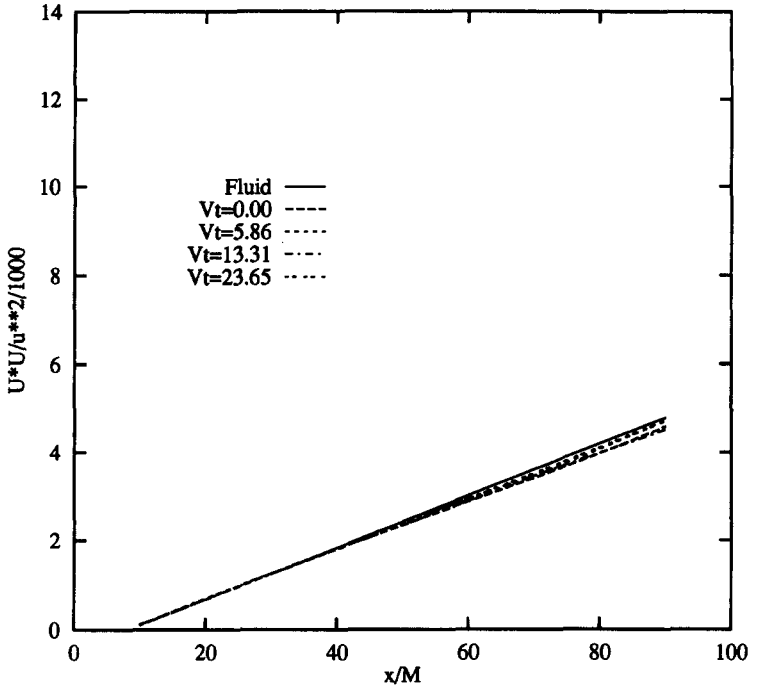

Figure 7b. Predicted transverse velocity decays of the 5 μm particles.

Tables 7 and 8 summarize the predicted values of τ_{ii}^{p} for the 5 and 57 μm particles, respectively. Here the subscript xx still denotes the longitudinal direction (the horizontal direction). For the case of $V_t = 0$ it can be deduced from the experiment that $\tau_{xx}^{p} = 19.6$ and $\tau_{xx}^{p} = 37.6$ (ms) for the 5 and 57 μm particles, respectively. The values predicted for this case are 25.03 and 38.35 (ms) for the 5 and 57 μm particles, respectively.

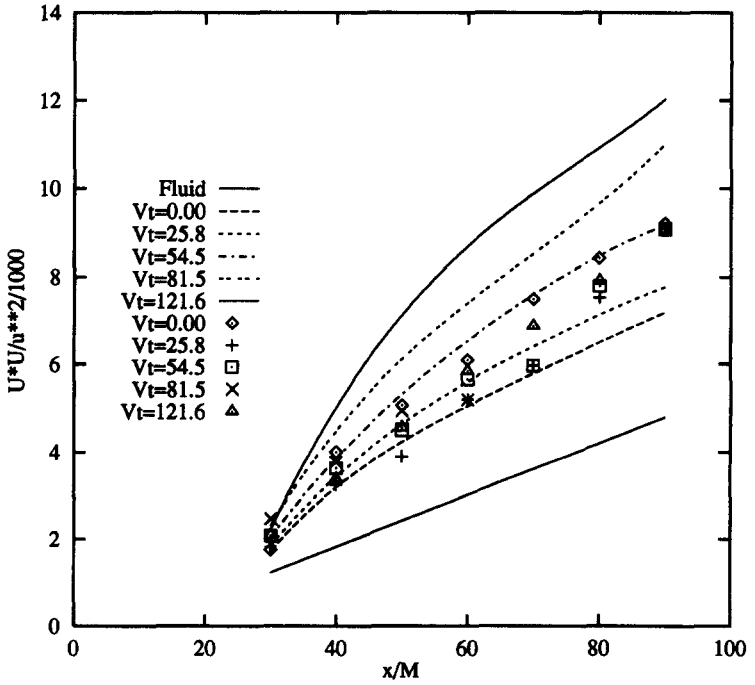

Figure 8a. Predicted and experimental longitudinal velocity decays of the 57 μm particles.

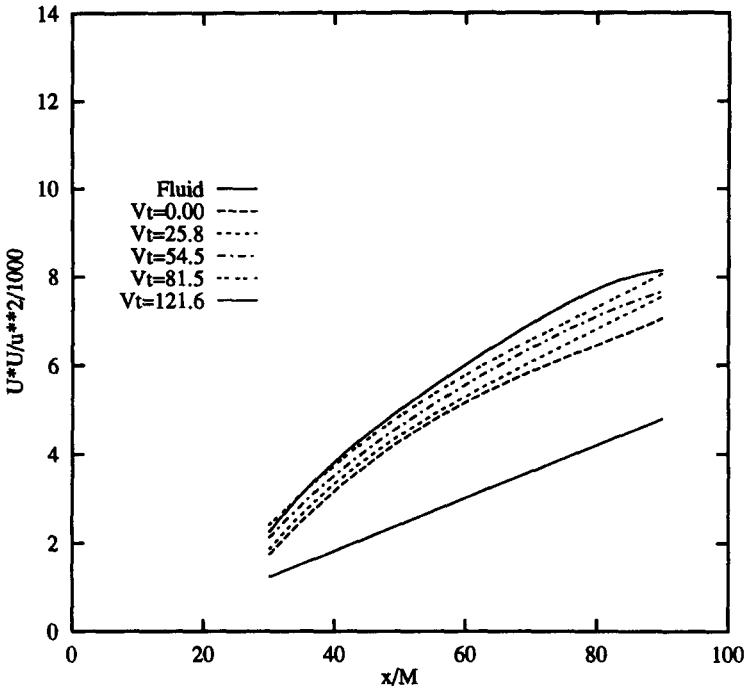

Figure 8b. Predicted transverse velocity decays of the 57 μm particles.

3.4. Sensitivity of model 1 to the time step Δt

Studies were also carried out to determine the sensitivity of the computed results to the choice of Δt. For this purpose, the experimental system of Snyder & Lumley (1971) was used to calculate the longitudinal and transverse particle diffusion coefficients, D_{11} and D_{22}. The computed results

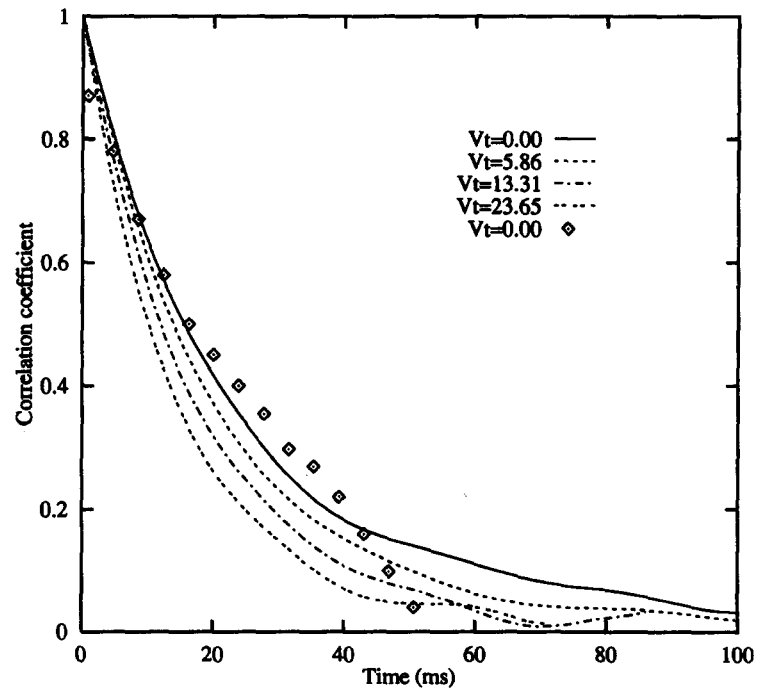

Figure 9a. Predicted Lagrangian longitudinal velocity correlations for the 5 μm particles as well as the experimental correlation in the case of $V_t = 0.0$.

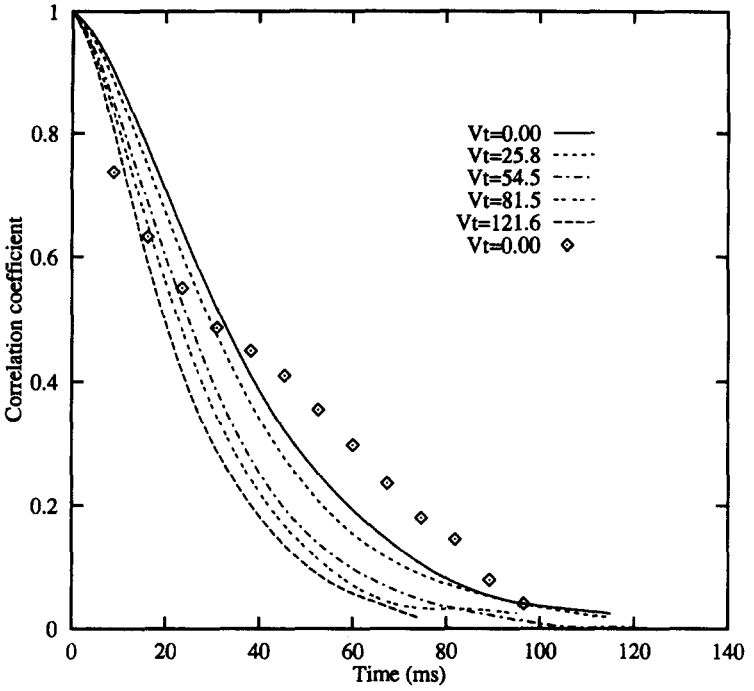

Figure 9b. Predicted Lagrangian longitudinal velocity correlations for the 57 μm particles as well as the experimental correlation in the case of $V_t = 0.0$.

are presented in table 9. The table also shows that the results are slightly dependent on the time step Δt. Our experience with the computation shows that in order to ensure good predictions, the following condition may be regarded as a conservative criteria for the time step Δt in model 1:

$$\Delta t = \min\left(\tau_1^L, \frac{\Lambda_1}{V_t}, \frac{\Lambda_2}{V_t}\right). \qquad [37]$$

3.5. Extension of model 1 to include the fluid Eulerian temporal correlations

As shown by the above predicted results, model 1 takes into account the crossing-trajectory effect and the continuity effect on the heavy particle dispersion, velocity decay and velocity correlation in the directions parallel and normal to the direction of gravity. However, in the absence of the crossing-trajectory effect, this model cannot give the prediction that the long-time particle diffusion coefficient is greater than fluid's. Reeks (1977) showed that this can occur only when the fluid Eulerian integral timescale is larger than the Lagrangian one. In stationary, homogeneous, isotropic and incompressible turbulence, Pismen & Nir (1978) directly related the long-time particle diffusion coefficient to the integral timescale of the fluid Eulerian temporal velocity correlation. This suggests that in order to predict that, in the absence of the crossing-trajectory effect, particles disperse more than the fluid, the inclusion of the fluid Eulerian temporal velocity correlation is necessary. In the following, model 1 is extended to include this correlation.

Table 7. 5 μm Particle data

V_t (cm/s)	τ_{xx}^P (ms)	τ_{yy}^P (ms)
0.00	25.03	22.60
2.73	20.48	23.29
5.86	21.04	23.86
13.31	19.26	19.12
17.06	15.70	18.67
20.91	14.88	18.12
23.65	15.01	19.36

Table 8. 57 μm Particle data

V_t (cm/s)	τ_{xx}^P (ms)	τ_{yy}^P (ms)
0.00	38.35	38.67
13.5	37.07	37.04
25.8	35.84	36.78
39.7	32.56	34.65
54.5	29.47	33.40
81.2	28.06	28.98
108.0	24.34	26.40
121.6	24.02	25.44

Table 9. Dependence of D_{11} and D_{22} on the time step Δt

	Hollow glass	Corn pollen	Glass	Copper
D_{11} [$\Delta t = 0.01$ (s)]	5.42	3.65	2.88	2.67
D_{22} [$\Delta t = 0.01$ (s)]	6.18	3.02	1.88	1.77
D_{11} [$\Delta t = 0.001$ (s)]	5.58	4.09	3.03	2.79
D_{22} [$\Delta t = 0.001$ (s)]	5.01	2.94	2.16	1.75
D_{11} [$\Delta t = 0.0001$ (s)]	5.66	3.58	2.93	2.91
D_{22} [$\Delta t = 0.0001$ (s)]	5.67	3.26	2.08	2.06

If turbulent flow has one principal mean flow direction, as is often the case in the experiments of Snyder & Lumley (1971) and Wells & Stock (1983) and the theoretical investigations of Reeks (1977), Pismen & Nir (1978) and Nir & Pismen (1979), there is another method of modeling the fluctuating fluid velocities at the positions $\mathbf{X}_s$ and $\mathbf{X}_p$, defined in figure 1. Let the mean flow direction be the x-direction and the mean velocity be U_m. The relative coordinate system O'–$\Theta'\Xi'\Omega'$, as shown in figure 10, is established. The origin of the coordinate system is at $\mathbf{X}_{o'}$ and the Θ' axis passes through the two positions $\mathbf{X}_{o'}$ and $\mathbf{X}_p$. In figure 10, $\mathbf{X}_{o'}$ is defined as $\mathbf{X}_s + U_m \Delta t \mathbf{i}$, where $\mathbf{i}$ is the unit vector of the absolute x axis. As in the discussion in subsection 2.2, the normalized fluctuating velocities of the fluid at positions $\mathbf{X}_s$, $\mathbf{X}_{o'}$ and $\mathbf{X}_p$ have the following correlation relations:

$$\overline{W_i(\mathbf{X}_{o'})W_j(\mathbf{X}_s)} = \overline{W_i(\mathbf{X}_s)W_j(\mathbf{X}_s)}\, F_{ij}^{E}(\Delta t) \quad (i,j = 1,2,3) \qquad [38]$$

and

$$\overline{W_i(\mathbf{X}_p)W_j(\mathbf{X}_{o'})} = \overline{W_i(\mathbf{X}_{o'}W_j(\mathbf{X}_{o'})}\, G_{ij}(\Delta s_1) \quad (i,j = 1,2,3). \qquad [39]$$

It is clear that [38] is the Eulerian temporal velocity correlation function in a frame of reference moving with the velocity U_m, because, seen from the coordinate system O'–$\Theta'\Xi'\Omega'$, $\mathbf{X}_s$ and $\mathbf{X}_{o'}$ occupy the same space point, as seen in theoretical works of Reeks (1977), Pismen & Nir (1978) and Nir & Pismen (1979). For this reason, this method is called the Eulerian temporal construction. The function G_{ij} is the same as g_{ij} in [4].

For reasons of simplicity, the normalized fluctuating fluid velocity in the coordinate system O'–$\Theta'[\Xi]'\Omega'$ is still denoted by W_i. Similarly, for isotropic turbulent flow cases, the following correlation relations hold:

$$\overline{W_i(\mathbf{X}_{o'})W_i(\mathbf{X}_s)} = \overline{W_i(\mathbf{X}_s)W_i(\mathbf{X}_s)}\, F_{ii}^{E}(\Delta t) \quad (i = 1,2,3) \qquad [40]$$

and

$$\overline{W_i(\mathbf{X}_p)W_i(\mathbf{X}_{o'})} = \overline{W_i(\mathbf{X}_{o'})W_i(\mathbf{X}_{o'})}\, G_{ii}(\Delta s_1) \quad (i = 1,2,3). \qquad [41]$$

For the fluctuating fluid velocities at the positions $\mathbf{X}_s$, $\mathbf{X}_{o'}$ and $\mathbf{X}_p$, it is postulated, respectively, that

$$W_i(\mathbf{X}_{o'}) = c_i W_i(\mathbf{X}_s) + \chi_i \quad (i = 1,2,3) \qquad [42]$$

and

$$_i(\mathbf{X}_p) = d_i W_i(\mathbf{X}_{o'}) + \delta_i \quad (i = 1,2,3), \qquad [43]$$

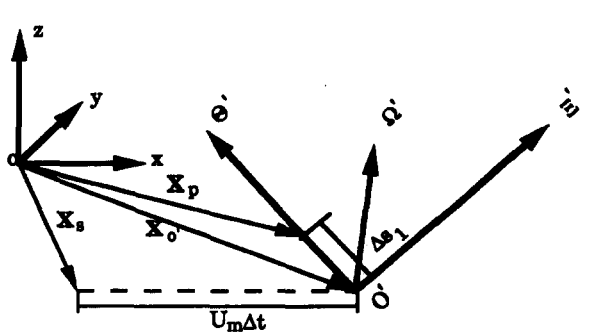

Figure 10. The coordinate system established for model 2.

where c_i, χ_i, d_i and δ_i $(i = 1, 2, 3)$ have the same sense as a_i, α_i, b_i and β_i in [7] and [10]. By similar procedures,

$$c_i = F_{ii}^{E}(\Delta t), \tag{44}$$

$$d_i = G_{ii}(\Delta s_1) \tag{45}$$

and

$$W_i(\mathbf{X}_p) = c_i d_i W_i(\mathbf{X}_s) + \zeta_i \quad (i = 1, 2, 3), \tag{46}$$

where $\zeta_i = c_i\chi_i + \delta_i$ $(i = 1, 2, 3)$ have the same meaning as ψ_i. Their standard deviations $(\sigma_\zeta)_i$ are

$$(\sigma_\zeta)_i = \sqrt{1 - c_i^2 d_i^2} \quad (i = 1, 2, 3). \tag{47}$$

Since [13] leads to the correct limiting result for fluid dispersion, the following relations are proposed in model 2:

$$W_i(\mathbf{X}_p) = \begin{cases} a_i b_i W_i(\mathbf{X}_s) + \psi_i & (i = 1, 2, 3) \quad \text{if } \Delta s_1 \geqslant R\Delta s \\ c_i d_i W_i(\mathbf{X}_s) + \zeta_i & (i = 1, 2, 3) \quad \text{if } \Delta s_1 < R\Delta s \end{cases} \tag{48}$$

Equation [48] is also called the mixed model in later discussions. Here R is an adjustable parameter. When $R = 0$, model 2 reduces to model 1. If $R = \infty$, the present model will be similar to that used by Reeks (1977) and Pismen & Nir (1978). As long as $R \neq \infty$, the resulting scheme will lead to the theoretical result of Taylor (1921) for the fluid dispersion coefficient. In the simulation of this subsection, simply $R = 1$. It should also be noted that the two alternative equations in [48] are not established in the same coordinate system.

Before validating model 2, some insight into its physical basis should be given. Two limiting situations can be considered. One is in the absence of the crossing-trajectory effect; the other is the case where the particle free-fall velocity is much larger than the turbulence intensity.

In the first case, when particle inertia is negligible, such as for a fluid point, particles can respond to all the turbulent fluctuations; thus $\Delta s \to 0$ and $\Delta s_1 \geqslant R\Delta s$ always holds. As a result, the first alternative in [48] controls the particle motion. In other words, particle motion is governed by its auto-correlation. This agrees with physical intuition. However, if particle inertia is so large that it remains immobile relative to the coordinate system moving with the velocity U_m, then the velocity correlation of the fluid at the particle position is the Eulerian temporal velocity correlation in the same frame of reference, as has been already pointed out by Pismen & Nir (1978). In this case, $\Delta s_1 \to 0$ in model 2. In fact, when $\Delta s_1 \to 0$, only the second alternative in [48] is used and $c_i d_i \to c_i$.

Another limiting case is when the particle free-fall velocity V_t is much larger than the turbulence intensity. Let V_t be directed in the negative direction of the absolute z-axis. Then the vector $\mathbf{X}_p - \mathbf{X}_f$ (see figure 1) and $\mathbf{X}_p - \mathbf{X}_{o'}$ can be expressed as $x'\mathbf{i} + y'\mathbf{j} + (z' - V_t\Delta t)\mathbf{k}$ and $x''\mathbf{i} + y''\mathbf{j} + (z'' - V_t\Delta t)\mathbf{k}$, respectively, where $\mathbf{i}$, $\mathbf{j}$ and $\mathbf{k}$ are the unit vectors of the x, y and z axes. When V_t is large enough so that x', y' and z' (or x'', y'' and z'') can be neglected, either $x'\mathbf{i} + y'\mathbf{j} + (z' - V_t\Delta t)\mathbf{k}$ or $x''\mathbf{i} + y''\mathbf{j} + (z'' - V_t\Delta t)\mathbf{k}$ can be approximated by $-V_t\Delta t\mathbf{k}$ in both alternatives in [48]. Consequently, the temporal (either Lagrangian or Eulerian) effect of the turbulence can be neglected in comparison to the spatial effect and $a_i b_i$ and $c_i d_i$ and $c_i d_i$ of [48] are equal to b_i and d_i. Since g_{ii} and G_{ii} are the same and they are approximately equal to $g_{ii}(V_t\Delta t)$, the velocity correlation of the fluid at the particle position now reduces to the Eulerian spatial correlation in the coordinate system moving with U_m in both alternatives in [48], regardless of the particle inertia. That is, when V_t is significant enough, models 1 and 2 are the same.

To verify model 2, a simulation for particle dispersion in a stationary, homogeneous, isotropic and incompressible turbulent flow is performed. This permits a comparison with the existing theoretical works of Csanady (1963), Pismen & Nir (1978) and Nir & Pismen (1979). In stationary, homogeneous, isotropic and incompressible turbulence, the turbulent variance, the Eulerian integral timescale and the Lagrangian integral timescale are independent of the reference direction. They are denoted by $\overline{u^2}$, τ^E and τ^L. The corresponding correlations take the following forms:

$$\overline{W_i(\mathbf{X}_{o'})W_i(\mathbf{X}_s)} = \overline{W_i(\mathbf{X}_s)W_i(\mathbf{X}_s)}\exp(-\Delta t/\tau_i^E) \qquad (i = 1, 2, 3), \tag{49}$$

and

$$\overline{W_i(\mathbf{X}_p)W_i(\mathbf{X}_{o'})} = \overline{W_i(\mathbf{X}_{o'})W_i(\mathbf{X}_{o'})}\exp(-\Delta s_1/2\Lambda_i)\cos(\Delta s_1/2\Lambda_i) \quad (i = 1, 2, 3). \tag{50}$$

A value is assigned to the ratio of the fluid Eulerian integral timescale to the Lagrangian, as done in the theoretical study of Pismen & Nir (1978). Pismen & Nir (1978) obtained an explicit expression for the long-time particle diffusion coefficient. Their result for a particle with a large time constant in the absence of the crossing-trajectory effect is

$$D_p = \tau^E \overline{u^2}. \quad [51]$$

As given by Taylor (1921), the long-time fluid diffusion coefficient D_f is

$$D_f = \tau^L \overline{u^2}. \quad [52]$$

According to Pismen & Nir's study, $D_p/D_f = 1.37$. Thus, from [51] and [52], $Ce_2 = \tau^E/\tau^L = 1.37$. So for the case of the stationary, homogeneous, isotropic and incompressible turbulent flow, calculations were conducted under the following mean turbulent flow conditions:

$$\overline{U_x} = 655 \text{ (cm/s)}, \quad \overline{U_y} = 0, \quad \overline{U_z} = 0, \quad [53]$$

$$\overline{u^2} = \overline{u_x^2} = \overline{u_y^2} = \overline{u_z^2} = 196 \text{ (cm}^2/\text{s}^2), \quad [54]$$

$$\tau^L = \tau_i^L = 32 \text{ (ms)} \quad (i = 1, 2, 3) \quad [55]$$

and

$$\tau^E = \tau_i^E = 1.37\tau^L \quad (i = 1, 2, 3). \quad [56]$$

The Eulerian spatial scales are defined as

$$\Lambda_1 = 2.5\tau^L \sqrt{\overline{u^2}} \quad [57]$$

and

$$\Lambda_2 = \Lambda_3 = 0.5\Lambda_1. \quad [58]$$

The turbulent mean velocity and variance given by [53]–[55] correspond to the values taken at the section $x/M = 68$ in the experiment of Synder & Lumley (1971). In the computation, particles were emitted at $x = 0$ and the initial particle velocity was set to be the local fluid instantaneous velocity. To avoid the effects of the initial condition, the statistics for particle dispersion began at $x = 900$ (cm).

For particle dispersion, situations could be distinguished. For one the crossing-trajectory effect is important; in the other it is not. In the former case, Csanady (1963) arrived at the following results for the long-time longitudinal and transverse diffusion coefficients of the particle, D_{11} and D_{22}:

$$D_{11} = \frac{L\overline{u^2}}{V_t}\left[1 + \frac{Ce_2^2\overline{u^2}}{V_t^2}\right]^{-1/2} \quad [59]$$

and

$$D_{22} = \frac{L\overline{u^2}}{V_t}\left[4 + \frac{Ce_2^2\overline{u^2}}{V_t^2}\right]^{-1/2}, \quad [60]$$

where L is defined as

$$L = \frac{\pi}{2\overline{u^2}} \int_0^\infty \frac{E(k)\,dk}{k} \quad [61]$$

and V_t the particle terminal velocity, is equal to $g\,\mathrm{Tp}$, where Tp is the particle time constant defined as below:

$$\mathrm{Tp} = \frac{\rho_f d_p^2}{18\rho_p \nu}.$$

$E(k)$ is the three-dimensional turbulent energy spectrum function. From turbulence theory, $L = \Lambda_1$ (e.g. Hinze 1975). It is clear from [59] and [60] that the crossing-trajectory effect reduces the particle dispersion rate, while the continuity effect makes particles disperse faster in the gravity direction

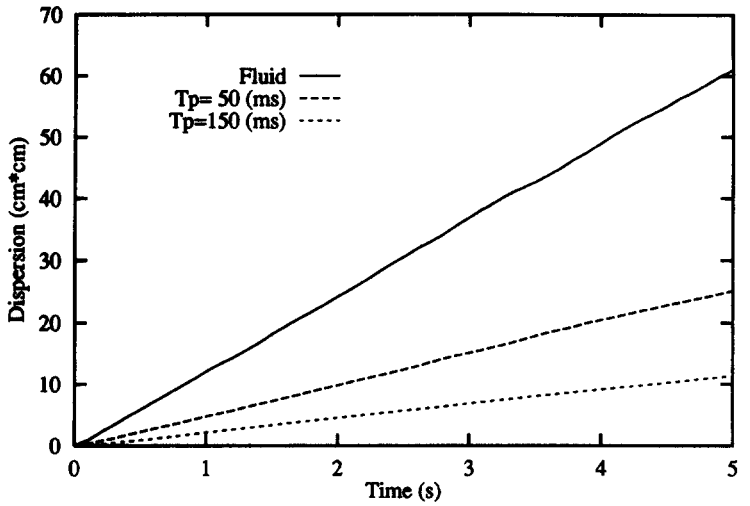

Figure 11a. Predicted longitudinal particle dispersions in the presence of the crossing-trajectory effect.

than in the normal direction. However, it should be pointed out that in the absence of V_t [59] and [60] are no longer valid, except in the limit of zero particle inertia. Formulas [59] and [60] are consistent with the works of Reeks (1977) and Pismen & Nir (1978) as $\overline{u^2}/V_t^2$ is small enough. Substituting the present values of A_1 and Ce_2 into [59] and [60], D_{11} and D_{22} are obtained. In the calculation, gravity is directed in the opposite direction to the x axis. Here the subscripts 11 and 22 represent the directions parallel and perpendicular to the gravitational force. Figures 11a and 11b represent the predicted dispersions for particles with different time constants Tp. Tables 10 and 11 give the predicted and theoretical (computed from [59] and [60]) long-time particle diffusion coefficients, respectively. It is observed from the two tables that with increasing Tp, the predicted values for D_{11}, D_{22} and D_{22}/D_{11} gradually approach the theoretical results given by [59] and [60]. This means that as long as $\sqrt{\overline{u^2}}$ is small enough, the predicted long-time particle diffusion coefficients D_{11} and D_{22} are inversely proportional to V_t and due to the continuity effect, D_{22}/D_{11} tends asymptotically to 0.5.

Another interesting case for the calculation of particle dispersion is when the effect of crossing-trajectories is absent. This allows an examination of the effect of particle inertia. Figure 12 gives computed particle dispersions for this case. Since the integral timescale of the Eulerian temporal velocity correlation is greater than the Lagrangian one in the present work, the long-time

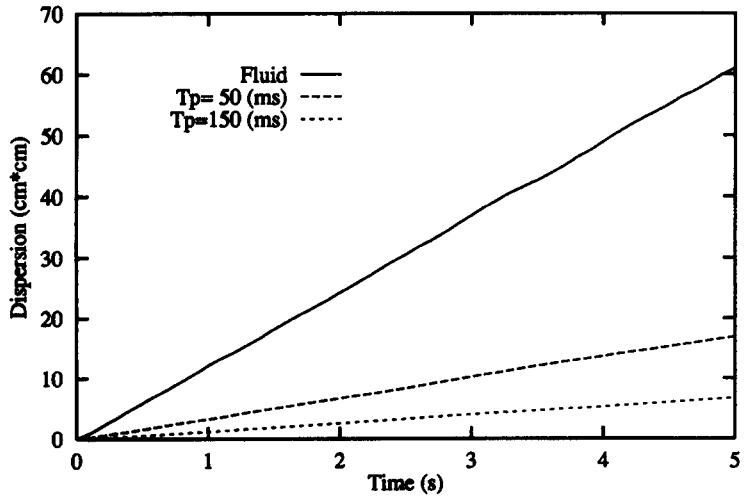

Figure 11b. Predicted transverse particle dispersions in the presence of the crossing-trajectory effect.

Table 10. Predicted long-time particle diffusion coefficients

Tp (ms)	50	150
D_{11} (cm^2/s)	2.51	1.16
D_{22} (cm^2/s)	1.63	0.66
D_{22}/D_{11}	0.65	0.57

Table 11. Theoretical long-time particle diffusion coefficients

Tp (ms)	50	150
D_{11} (cm^2/s)	3.65	1.46
D_{22} (cm^2/s)	2.11	0.74
D_{22}/D_{11}	0.58	0.51

particle diffusion coefficient increases with the particle time constant; it is larger than that of the fluid, as explained by Reeks (1977). This is shown clearly in figure 12. The predicted long-time particle diffusion coefficients for the 1600 (ms) particle and fluid are, respectively, 9.1 and 6.0 (cm^2/s). Their theoretical counterparts are 8.59 and 6.272 (cm^2/s), given by [51] and [52], respectively. The two are in a fair agreement. The restriction on the timestep of model 2 is

$$\Delta t = \min\left(\tau_1^L, \tau_1^E, \frac{\Lambda_1}{V_t}, \frac{\Lambda_2}{V_t}\right). \qquad [62]$$

4. DISCUSSION AND CONCLUSIONS

Based on the idea of a time series analysis (Box & Jenkins 1976), two Lagrangian models, that include the effects of the temporal and spatial variations of the turbulence on particles, have been established. Model 1 is used to simulate particle dispersion in the two grid-generated decaying isotropic turbulent air flows studied by Snyder & Lumley (1971) and Wells & Stock (1983). Comparison is made of the predicted and measured particle dispersion and velocity decay in the transverse direction. Computed particle dispersion and velocity decay are also presented for the longitudinal direction. The crossing-trajectory and continuity effects can be observed clearly on the particle dispersion and velocity decay. The numerical results are also compared with the theoretical results of Nir & Pismen (1979) for the copper particle velocity auto-correlation of the experiment of Snyder & Lumley (1971). In addition, in order to examine the combined effects of inertia, continuity and crossing-trajectories, the integral timescales of particle auto-correlations are given in the directions parallel and normal to gravity. Some comparisons are in good agreement and others are not. For example, model 1 underpredicts the 57 μm particle dispersions for the experiment of Wells & Stock (1983) and it cannot show that 57 μm particles disperse faster than 5 μm particles when $V_t = 0$. The sensitivity of model 1 to the time step Δt of the computation was tested; the results indicate that particle dispersion depends only slightly on Δt.

In the case where the turbulent mean flow has one main direction, model 1 has been extended to include the Eulerian temporal velocity correlation and the so-called mixed model (model 2) has

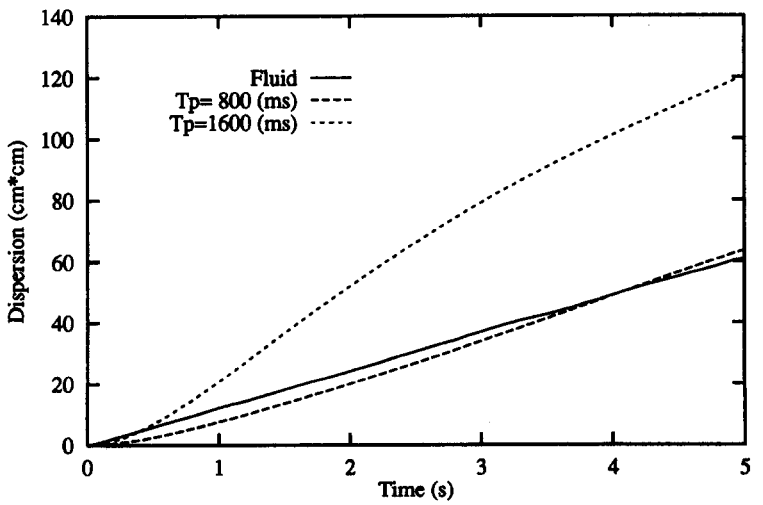

Figure 12. Predicted particle dispersions in the absence of the crossing-trajectory effect.

been devised. The mixed model is then applied to particle dispersion in a stationary, homogeneous, isotropic and incompressible turbulent flow. The numerical results show that model 2 is capable of predicting, in the absence of the crossing-trajectory effect, that the long-time particle diffusion coefficient is larger than that of the fluid if the Eulerian integral timescale of the velocity correlation is larger than the Lagrangian one, as pointed out by Reeks (1977). The long-time particle and fluid diffusion coefficients computed by model 2 agree with the theoretical results of Pismen & Nir (1978) and Taylor (1921), respectively. It is also verified that when the particle drift is dominant, the predicted long-time longitudinal and transverse particle coefficients gradually approach the two formulas of Csanady (1983); i.e. the long-time particle diffusion coefficient in the gravity direction is twice the transverse one and that both diffusion coefficients are inversely proportional to the particle free-fall velocity. This implies that model 2 takes into account inertia, continuity and crossing-trajectory effects. However, if V_t is small, the long-time particle diffusion coefficient given by the present study disagrees somewhat with Csanady's result.

Furthermore, calculations, not presented here, show that, except for the case where the crossing-trajectory effect is absent and the particle time constant is large, the differences between the results arising from models 1 and 2 are insignificant.

All the calculations presented above were obtained by averaging over 5000 particles trajectories on a SUN SPARC 1 station. For a typical run, the particle dispersions shown in figures 2a and 2b, required about 1800 CPU seconds.

Acknowledgements—Thanks are given to Professor H. Burnage (Institute de Mécanique des Fluides de Strasbourg, France) and Professor T. J. Hanratty, as well as to the five other referees, for their helpful and illuminating comments which have led to the significant improvement of this study.

REFERENCES

ABBAS, A. S., KOUSSA, S. S. & LOCKWOOD, F. C. 1980 The prediction of particle laden gas flow. Report FS/80/1, ICST, London.

BERLEMONT, A., DESJONQUERES, P. & GOUESBET, G. 1990 Particle Lagrangian simulation in turbulent flows. *Int. J. Multiphase Flow* **16,** 19–34.

BOX, G. E. P. & JENKINS, G. M. 1976 *Time Series Analysis.* Holden-Day, Oakland, CA.

BURNAGE, H. & MOON, S. 1990 Prédétermination de la dispersion de particules matérielles dans un écoulement turbulent. *C.R. Acad. Sci. Paris Ser. II* **310,** 1595–1600.

CSANADY, G. T. 1963 Turbulent diffusion of heavy particles in atmosphere. *J. Atmos. Sci.* **20,** 201–208.

DURBIN, P. A. 1980 A stochastic model for two-particle dispersion and concentration fluctuations in homogeneous turbulence. *J. Fluid Mech.* **100,** 279–302.

DURST, F., MILOJEVIC, D. & SCHONUNG, B. 1984 Eulerian and Lagrangian predictions of particulate two-phase flows: a numerical study. *Appl. Math. Modelling* **8,** 101–115.

ELGHOBASHI, S. E., ABOU ARAB, T. W., RIZK, M. & MOSTAFA, A. 1984 Prediction of the particle-laden jet with a two equation turbulent model. *Int. J. Multiphase Flow* **10,** 697–710.

FRENKIEL, F. N. 1948 Etude statistique de la turbulence-fonctions spectrales et coefficients de corrélation. Rapport Technique, ONERA No. 34.

GOSMAN, A. D. & IOANNIDES, E. 1981 Aspects of computer simulation of liquid-fuelled combustors. Paper presented at the *AIAA 19th Aerospace Science Mtg*, St. Louis, MO, Paper 81–0323.

HINZE, H. O. 1975 *Turbulence.* McGraw-Hill, New York.

KALLIO, G. A. & REEKS, M. W. 1989 A numerical simulation of particle deposition in turbulent boundary layers. *Int. J. Multiphase Flow* **15,** 433–446.

KAPLAN, H. & DINAR, N. 1988 A three-dimensional stochastic model for concentration fluctuation statistics in isotropic homogeneous turbulence. *J. Comput. Phys.* **79,** 317–335.

NIR, A. & PISMEN, L. M. 1979 The effect of a steady drift on the dispersion of a particle in turbulent fluid. *J. Fluid Mech.* **94,** 369–381.

ORMANCEY, A. 1984 Simulation du comportement de particule dans des écoulements turbulents. Thèse de 3eme cycle, Ecole de Mines de Paris.

ORMANCEY, & MARTINON, A. 1984 Prediction of particle dispersion in turbulent flows. *Physico Chem. Hydrodynam.* **5,** 229–240.

PARTHASARATHY, R. N. & FAETH, G. M. 1990 Turbulent dispersion of particles in self-generated homogeneous turbulent. *J. Fluid Mech.* **220,** 515–537.

PISMEN, L. M. & NIR, A. 1978 On the motion of suspended particles in stationary homogeneous turbulence. *J. Fluid Mech.* **84,** 193–206.

REEKS, M. W. 1977 On the dispersion of small particles suspended in an isotropic turbulent fluid. *J. Fluid Mech.* **83,** 529–546.

RUBINOW, S. I. & KELLER, J. B. 1961 The transverse force on a spinning sphere moving in a viscous fluid. *J. Fluid Mech.* **11,** 447–459.

SAFFMAN, P. G. 1965 The lift on a small sphere in a slow shear flow. *J. Fluid Mech.* **22,** 385–400.

SAWFORD, B. L. & HUNG, J. C. R. 1986 Effects of turbulence structure, molecular diffusion and source size on scale fluctuations in homogeneous turbulence. *J. Fluid Mech.* **165,** 373–400.

SHUEN, J. S., CHEN, L. D. & FAETH, G. M. 1983 Evaluation of a stochastic model of particle dispersion in a turbulent round jet. *AIChE Jl* **29,** 167–170.

SHUEN, J. S. SOLOMON, A. S. P., ZHANG, Q. F. & FAETH, G. M. 1985 Structure of particle-laden jets: measurements and predictions. *AIAA Jl* **23,** 396–404.

SNYDER, W. H. & LUMLEY, J. L. 1971 Some measurements of particle velocity autocorrelation functions in a turbulent flow. *J. Fluid Mech.* **48,** 41–71.

TAYLOR, G. I. 1921 Diffusion by continuous movements. *Proc. R. Soc. Ser. A* **20,** 196–211.

VETTERLING, W. T., TEUKOLSKY, S. A., PRESS, W. H. & FLANNERY, B. P. 1988 *Numerical Recipes Example Book.* Cambridge University Press, Cambridge, U.K.

WAX, N. 1954 *Selected Papers on Noise and Stochastic Processes.* Dover, New York.

WELLS, M. R. & STOCK, D. E. 1983 The effects of crossing trajectories on the dispersion of particles in a turbulent flow. *J. Fluid Mech.* **136,** 31–62.